J Herbmed Pharmacol. 2023; 12(4): 469-482.

http://www.herbmedpharmacol.com doi: 10.34172/jhp.2023.44672

Journal of Herbmed Pharmacology

Phytochemical profiling, pharmacology prediction, and molecular docking study of *Chromolaena odorata* extract against multiple target proteins in wound healing

Nur 'Ainun Mokhtar[1,2*], Fatahiya Mohamed Tap[3], Nur Hannani Ahmad Rozani[3], Nurul Bahiyah Ahmad Khairudin[2*], Roshafima Rasit Ali[2]

[1]Faculty of Pharmacy, UiTM Cawangan Pulau Pinang, Kampus Bertam, 13200 Kepala Batas, Pulau Pinang, Malaysia
[2]Malaysia-Japan International Institute of Technology, Universiti Teknologi Malaysia, International Campus, Jalan Sultan Yahaya Petra, 54100 Kuala Lumpur, Malaysia
[3]School of Chemical Engineering, College of Engineering, Universiti Teknologi MARA Cawangan Terengganu, Kampus Bukit Besi, 23200 Dungun, Terengganu, Malaysia

ARTICLE INFO

Article Type:
Original Article

Article History:
Received: 20 October 2022
Accepted: 30 March 2023

Keywords:
Squalane, Gas chromatography-mass spectrometry, Drug design, Glycogen synthase kinase 3 beta, Cyclooxygenase 2 inhibitor, Matrix metalloproteinase 9

ABSTRACT

Introduction: Wounds have a significant influence on socioeconomic and the quality of life. Many attempts have been taken to produce advanced wound dressing to fulfill demands. The incorporation of natural therapeutics like medicinal plants in wound dressings is currently popular. However, several medications have failed to enter the market due to inadequate pharmacokinetics data. Computer-aided tools are now available as advanced drug discovery methods, which can be used to screen pharmaceuticals from phytochemicals found in various medicinal plants. This study aims to evaluate the phytoconstituents of *Chromolaena odorata* extract and its pharmacological potential as a wound-healing agent.

Methods: Phytoconstituents from *C. odorata* were identified using qualitative screening methods and gas chromatography-mass spectrometry (GC-MS), and their mechanistic properties were assessed using molecular docking and SwissADME tools.

Results: Current works revealed that the topmost phytoconstituents in *C. odorata* were phytol (49.83%), hexadecanoic acid ethyl ester (9.40%), linolenic acid (8.07%), and squalene (3.53%). Through SwissADME analysis, all four topmost compounds obeyed Lipinski's Rule of 5. *In silico* molecular docking study of these top phytoconstituents against several protein targets involved in wound healing revealed that squalene had the highest binding affinity to GSK3-β (-6.8 kJ/mol), MMP-9 (-7.4 kJ/mol), and COX-2 (-8.6 kJ/mol) as compared to other ligands (phytol, linolenic acid, and hexadecenoic acid ethyl ester).

Conclusion: These findings suggest that the most prominent compound that contributes to *C. odorata*'s wound healing capacity is squalene and the incorporation of *C. odorata* in potential wound dressing formulation is justified.

Implication for health policy/practice/research/medical education:
This study provides insight into *Chromolaena odorata*'s valuable phytochemical compounds. Molecular docking as well as adsorption, distribution, metabolism, and excretion (ADME) prediction performed in this study provide more evidence of *C. odorata*'s wound-healing potential by elucidating its inhibitory activity against pivotal protein targets during the inflammation, proliferation, and remodeling stages of wound healing. The information presented in this paper serves as preliminary data for any wound healing product planned to be prepared with *C. odorata* extracts or any of its phytoconstituents.

Please cite this paper as: Mokhtar NA, Mohamed Tap F, Ahmad Rozani NH, Ahmad Khairudin NB, Rasit Ali R. Phytochemical profiling, pharmacology prediction, and molecular docking study of *Chromolaena odorata* extract against multiple target proteins in wound healing. J Herbmed Pharmacol. 2023;12(4):469-482. doi: 10.34172/jhp.2023.44672.

***Corresponding authors**: Nur 'Ainun Mokhta, Email: nurain2942@uitm.edu.my, Bahiyah Ahmad Khairudin, Email: r-bahiah@utm.my

Introduction

Globally, wound-related problems have a major impact on socioeconomic. A 2018 market research report predicted that the global wound-closure products market will exceed $15 billion by 2022 (1). Even though most wound-related problems do not always involve hospitalizations, it is still having major consequences when the wound comes to healing. Traditionally, various methods have been utilized by many cultures throughout the world, such as honey pastes, animal fats, as well as herbal preparations as wound healing remedies. Herbal medicines are usually comprised of a mixture of various phytochemicals used to treat contagious and prolonged diseases (2,3). Characterization of various bioactive compounds from medicinal plants has resulted in the development of important medicines (4). However, many examined drugs could not enter market due to their poor pharmacokinetic properties (5). Computational prediction tools are advanced methods used in pharmaceutical drug discovery. They are usually employed to predict the pharmacokinetics, pharmacological, and toxicological properties of drugs via *in silico* approaches (6,7). Molecular docking has gained popularity for testing and designing drugs. This tool can provide important information about drug receptor interactions useful for predicting the binding orientation of drugs to their target receptors (7). Furthermore, drug pharmacokinetics can be predicted for adsorption, distribution, metabolism, and excretion (ADME) of drugs via computational tools. In early drug discovery, ADME prediction is important to evaluate drug candidates for safety and efficacy, which are crucial for regulatory approval (8).

Pursuing the development of potential wound healing agent, the molecular drug target needs to be identified. Based on the existing studies, downregulation of proteins, in particular biochemical pathway, might have a significant role in targeting wound healing therapy (9,10). Based on the available literature, among protein targets that have been investigated to be responsible in wound healing are glycogen synthase kinase 3β (GSK3-β) (11,12), matrix metalloproteinase 9 (MMP-9) (13), and acylated human cyclooxygenases (COX-2) (14). In the current study, we aimed to evaluate the major phytochemical constituents from a local medicinal plant, *Chromolaena odorata* and subsequently elucidate its pharmacokinetics attributes as drug candidate through ADME prediction. Additionally, the major phytoconstituents of *C. odorata* was further investigated for their interaction against several target proteins that responsible in wound healing process via molecular docking approach.

Materials and Methods

Plant verification

The plant was collected from palm oil plantation in Felda Sg Kemahal, Pahang. The leaves were clean thoroughly with tap water to remove impurities and dirt. The whole plant was air dried to remove excess moisture. The fresh plant was kept as herbarium specimen and sent for verification by certified botanist in Biodiversity Unit, Institute of Bioscience, Universiti Putra Malaysia (Sample voucher: KM0013/22).

Plant extraction

The fresh leaves of *C. odorata* was separated from other aerial parts prior to extraction process. The ethanolic extract of *C. odorata* were obtained by soaking 10g of dried leaves of *C. odorata* in 150 mL of ethanol. The leaves were ultrasonicated for 10 minutes and macerated for 24 hours at room temperature. The extracts were filtered through Whatman #1 filter paper and further concentrated under vacuum forming dark brownish green paste. The paste was stored at -4°C until further use.

Phytochemical screening

Plant ethanolic extract obtained were then evaluated for the presence of terpenoids, steroids, flavonoids, alkaloids, saponins and tannins using method as described below (15).

Test for terpenoids: In a 5 mL test tube, 1 mL of chloroform were added to 5 mL of the extract and 3 mL of concentrated H_2SO_4. The presence of terpenoids was shown by the interface turning reddish brown.

Test for steroid: 0.5 mL of acetic anhydride and few drops of the concentrated H_2SO_4 were mixed with 1 mL of the extract, and a bluish-green precipitate confirmed the presence of steroids.

Test for flavonoids: 1 mL of extract was added to a 5 mL test tube for the flavonoids test. Then, 2 mL of 10% NaOH were added. The presence of flavonoids was demonstrated by the colour change from yellow to colourless when weak hydrochloric acid was added.

Test for alkaloids: 1 mL of Wagner's reagent was added to a mixture of 2 mL chloroform and 1 mL of extract to test for alkaloids. The presence of alkaloids was indicated by a reddish-brown precipitate.

Test for saponins: 1 mL of the extract was mixed with 5 mL of distilled water in test tube and shaken. Persistence foaming indicated the presence of saponins.

Test for tannins: 1 mL of extract was transferred into a 5 mL test tube. Then, approximately three drops of 5% iron (III) Chloride were added to the extract. A greenish black precipitate showed the presence of tannins.

Gas chromatography mass spectroscopy (GC-MS)

The collected extract was further subjected to GC-MS analysis performed on an Agilent 7890B gas chromatography system (Agilent, CA, USA) coupled with Agilent 5975C (Agilent, CA, USA) mass selective detector and fitted with DB-1MS column (30 m × 0.25 mm x 0.25 μm). Helium was used as the carrier gas at a flow rate of

1.0 mL/min under the following operating conditions: 2mL initial injection volume, split injection ratio of 1:10, initial oven temperature stabilisation at 60°C for 4 minutes and ramping to 230°C at a rate of 6°C/min, detector temperature of 260°C, injector temperature of 230°C and ionisation voltage of 70 eV. The chemical components in the extract were identified and quantified by comparing the mass spectra to the NIST library database.

In silico ADME analysis (drug-likeness evaluation)

The drug-likeness evaluation of selected compounds obtained by GC-MS from *C. odorata* ethanolic extract were performed using SwissADME webtool (https://www.swissadme.ch/). SwissADME is a free open access tool developed by Swiss Institute of Bioinformatics (SIB). In this current investigation, SMILE canonical data was used as the input parameter which was obtained from PubChem database (https://www.pubchem.com/) for top four compounds of *C. odorata* analysed by GC-MS. The ADME of the respective phytoconstituents were evaluated based on their physicochemical properties, lipophilicity, water solubility and pharmacokinetics characteristics obtained from SwissADME tools. The drug-likeness of the phytoconstituents were also being evaluated based on Lipinski's Rule of 5, Veber, Ghose, Egan and Muegge.

Molecular docking study and visualization

Protein Data Bank (PDB) was used to retrieve the 3D structure of GSK-3β (PDB ID: 1Q5K), MMP-9 protein (PDB ID: 4H1Q) and acetylated human COX-2 (PDB ID:5F19). These protein targets were selected based on the literature search of significant protein target in wound healing activities (11,16-18). PyMOL programme was used to remove all water molecules, ions, and ligands. The protein structures were then stored in PDB format for further analysis. Each phytochemical's 3D structure (phytol, squalene, linolenic acid and hexadecenoic acid ethyl ether) was downloaded in SDF format from PubChem. The Online Smiles Translator was then used to convert each structure into PDB format. The 3D structure of the reference molecule was also retrieved from PubChem in SDF format and converted to PDB using Online Smiles Translator. AMDock (19) was used to perform molecular docking of four phytochemicals against 1Q5K, 4H1Q and 5F19. AMDock has several programs/scripts that help to speed up the preparation procedure while maintaining control over the docking environment. To acquire binding location for specific site docking, the grid box was generated using AutoDock Tools as shown in Table 1.

To begin, a reference molecule was docked to validate the docking technique. As a result, the four phytochemicals were docked to the glycogen target site and the binding energy was extracted from the software. The interactions between the ligands and the target protein were observed and analysed. For molecular docking visualization, the Discovery Studio software was used to analyse molecular interactions between the protein-ligand structure and binding mode.

Table 1. Parameters used for molecular docking study

Protein target	PDB ID	Grid box coordinate	Grid Box Size
GSK3-β	1Q5K	X=23.9, Y=19.9 Z=7.6	34 x 34 x 34
MMP-9	4H1Q	X=29.2, Y= 0.0, Z= 23.8	33 x 33 x 33
COX-2	5F19	X=23.9, Y=19.9, Z=7.6	34 x 34 x 34

GSK3-β, Glycogen synthase kinase 3-β; MMP-9, Matrix metalloproteinase 9; COX-2, Cyclooxygenase 2.

Results

Phytochemical screening

Based on the preliminary phytochemical screening, the ethanolic extract of *C. odorata* showed the presence of several secondary metabolites including terpenoids, steroids, flavonoids, alkaloids, saponin, and tannins (Table 2). Based on the current work, qualitatively, terpenoids, flavonoids, alkaloids, and tannins were highly present while steroids and saponins showed lesser existence.

GC-MS analysis

GC-MS analysis was employed to tentatively identify the chemical compounds in the *C. odorata* ethanolic extract (Figure 1). Based on the current GC-MS analysis (Table 3), *C. odorata* leaves were rich of fatty acids, terpenes, and alkene. In comparison, a previous investigation on *C. odorata* leaves from Ivory Coast (20) showed that the extract contained geigerene (11.68%), α-pinene (21.15%), and pregeigerene (19.61%); from Thailand (21), this plant was reported to be comprised of geigerene (3.1%), α-pinene (20.7%) and pregeigerene (17.6%); from Nigeria (22) it was comprised of germacrene D (9.7%), α-pinene (42.2%), (E)-caryophyllene (5.4%), β-copaen-4α-ol (9.4%), pregeijerene/geijerene (7.5%), and β-pinene (10.6%). These previous results showed clear variations in the results of this study whereby phytol (49.83%), hexadecanoic acid ethyl ester (9.40%), linolenic acid (8.07%) and squalene (3.53%) are the topmost phytoconsitituents.

Table 2. Phytochemicals screening of *Chromolaena odorata* ethanolic extract

Phytochemicals	Presence
Terpenoids	++
Steroids	+
Flavonoids	++
Alkaloids	++
Saponins	+
Tannins	++

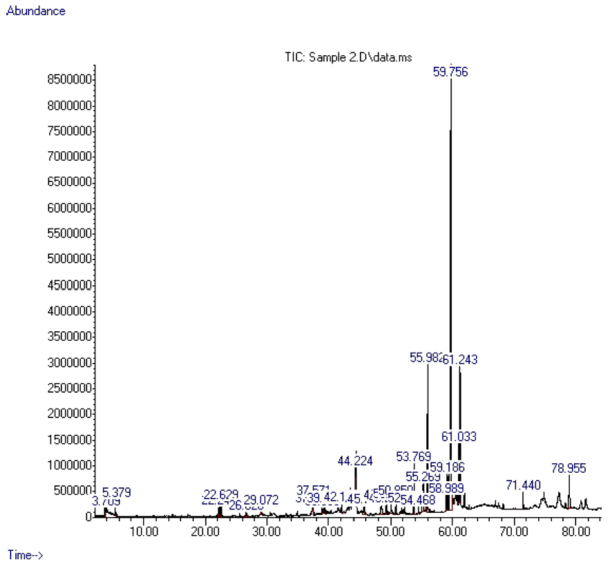

Figure 1. Total ion current plot of *Chromolaena odorata* ethanolic extract from GC-MS analysis.

Table 3. Chemical composition of *Chromolaena odorata* ethanolic extract based on GC-MS analysis

Compounds	Area (%)	Quality (%)
Trimethylsilylamine, N-(4-bromobenzylidene)	0.33	53
2-Phenyl-4-ethylidene-2-oxazolin-5-one	0.58	50
Cyclohexene, 3,4-diethenyl-3-methyl	0.91	74
4H-Pyran-4-one, 2,3-dihydro-3,5-dihydroxy-6-methyl	1.51	83
Benzofuran, 2,3-dihydro-	0.67	56
Benzene, 1-(1,1-dimethylethyl)-3-ethyl	0.49	70
1,6-Cyclodecadiene, 1-methyl-5-methylene-8-(1-methylethyl)-, [s-(E,E)]	0.33	98
1H-Cyclopenta[1,3]cyclopropa[1,2]benzene, octahydro-7-methyl-3-methylene-4-(1-methylethyl)-,[3aS-(3a. alpha., 3b.beta., 4.beta., 7.alpha., 7aS*)]	0.93	97
Naphthalene	0.79	97
Diethyl Phthalate	0.50	98
2-Naphthalenemethanol	1.96	99
Cycloisolongifolene	0.59	45
Dodecyl acrylate	0.54	60
5-Ethylcyclopent-1-ene-1-carboxylic acid	1.98	30
1-Octadecene	0.60	95
2-Naphthalenemethanol	1.08	50
9-Octadecyne	0.95	49
1,13-Tetradecadiene	0.54	58
Hexadecanoic acid, methyl ester	2.68	98
Isophytol	0.41	91
n-Hexadecanoic acid	3.17	98
Hexadecanoic acid, ethyl ester	9.40*	98
9,12-Octadecadienoic acid (Z,Z)-, methyl ester	0.95	99
9,12,15-Octadecatrienoic acid, methyl ester, (Z,Z,Z)-	2.26	99
Phytol	49.83*	91
9,12-Octadecadienoic acid	3.36	99
Linolenic Acid	8.07*	99
Phthalic acid, dodecyl octyl ester	1.09	64
Squalene	3.53*	99

* Indicates the topmost compounds.
Area (%) refers to the quantity.
Quality value was auto-generated by the GC-MS instrument and represents how well the detection was at that peak.

In silico ADME evaluation

Based on the GC-MS result, the four topmost compounds detected from *Chromolaena odorata* were further subjected to assessment on its drug-likeness behaviour through ADME prediction. The evaluation was conducted *in silico* using SwissADME Webtool (http://www.swissadme.org). Table 4 represents the physicochemical properties of the selected phytoconstituents of *Chromolaena odorata*.

Table 5 summarises the lipophilicity of topmost compounds from *C. odorata*. SwissADME provides five freely available models for determining a compound's lipophilicity: XLOGP3, WLOGP, MLOGP, SILICOS-IT, and iLOGP. XLOGP3 is an atomistic technique that incorporates corrective elements and a knowledge-based library (23). WLOGP is a purely atomistic method for analysing a fragmented system. MLOGP, a forerunner of the topological technique, is based on a linear relationship with the implementation of 13 molecular descriptors. SILICOS-IT is a hybrid algorithm that employs 27 fragments and seven topological descriptors. iLOGP is a physics-based approaching that calculates solvation free energy in n-octanol and water using the generalized-born and solvent accessible surface area (GB/SA) models. The consensus log P o/w is the arithmetic mean of the values anticipated by the five proposed approaches.

Table 6 represents the pharmacological attributes of the selected compounds of *Chromolaena odorata*. SwissADME adopts support vector machine algorithm for the datasets of known substrates/non-substrates or inhibitors/non-inhibitors for binary classifications (23). The tested molecules will give "Yes" or "No" for the molecule under investigation if they are expected to be either substrate for P-gp and CYP isozymes.

Drug-likeness is another feature in SwissADME that quantitatively examines how closely the compounds' physicochemical and structural attributes resemble those of well-known medications on the available database. Table 7 represents the computational drug-likeness of the selected compounds in *C. odorata* based on the "Rule of five" filters– Lipinksi's (Pfizer), Ghose (Amgen), Verber (GSK), Egan (Pharmacia), and Muegge (Bayer). As depicted in Table 7, all compounds are in compliance with Lipinski's rule (not more than 1 violation of the

Table 4. Physicochemical properties of selected compounds of *Chromolaena odorata*

Compound	Formula	MW	NHD	NHA	Rotatable bond	TPSA
Phytol	$C_{20}H_{40}O$	296.53	1	1	13	20.23
Hexadecanoic acid, ethyl ester	$C_{18}H_{36}O_2$	284.48	0	2	16	26.30
Linolenic Acid	$C_{20}H_{34}O_2$	306.48	0	2	15	26.30
Squalene	$C_{30}H_{50}$	410.72	0	0	15	0.00

MW: Molecular weight; NHD: Number of hydrogen donor; NHA: Number of hydrogen acceptor; TPSA: Topological polar surface area.

Table 5. Lipophilicity of selected compounds of *Chromolaena odorata*

Compound	Models*					
	iLOGP	XLOGP3	WLOGP	MLOGP	SILICOS-IT	Consensus log $P_{o/w}$
Phytol	4.71	8.19	6.36	5.25	6.57	6.22
Hexadecanoic acid, ethyl ester	4.65	7.88	6.03	4.67	6.28	5.9
Linolenic acid	5.03	7.34	6.36	4.93	6.80	6.09
Squalene	6.37	11.58	10.60	7.93	10.41	9.38

* SwissADME models for determining a compound's lipophilicity. iLOGP is a physics-based approach that calculates solvation-free energy in n-octanol and water. XLOGP3 is an atomistic technique. WLOGP is a purely atomistic method. MLOGP is a forerunner of the topological technique. SILICOS-IT is a hybrid algorithm technique. The consensus log $P_{o/w}$ is the arithmetic mean of the values anticipated by the five proposed approaches.

Table 6. Pharmacokinetics of the selected compounds of *Chromolaena odorata*

Parameters	Phytol	Hexadecanoic acid ethyl ester	Linolenic acid	Squalene
GI absorption	Low	High	High	Low
BBB permeant	No	No	No	No
P-gp substrate	Yes	No	No	No
CYP1A2 inhibitor	No	Yes	Yes	No
CYP2C19 inhibitor	No	No	No	No
CYP2C9 inhibitor	Yes	No	Yes	No
CYP2D6 inhibitor	No	No	No	No
CYP3A4 inhibitor	No	No	No	No
Log K_p (skin permeation)	-2.29	-2.44	-2.97	-0.58

parameters). However, all other four filters (Ghose, Verber, Egan, and Muegge) showed violations. Nevertheless, all of these compounds returned zero pan-assay interference compounds (PAINS) alert.

Figure 2 represents the bioavailability radar of the four topmost compounds of *Chromolaena odorata*. This 2D diagram is a unique feature generated by SwissADME tools and give an early insight at the drug-likeness of a molecule. The pink area represents the optimal range for each property. According to Daina et al (23), through bioavailability radar, the compound must fall within the range of the followings: XLOGP3 between – 0.7 and + 5.0, size: MW between 150 and 500 g/mol, polarity: TPSA between 20 and 130 Å 2 , solubility: log S not higher than 6, saturation: fraction of carbons in the sp 3 hybridization not less than 0.25, and flexibility: no more than 9 rotatable bonds.

Molecular docking analysis

The relationship between the compounds and the receptor plays a vital role in any formulations of drugs. Given the rise in drug resistance of numerous diseases and portentous side effects of conventional therapies, plant-based medications offer justifiable solutions. In this direction, the topmost active ingredients of *C. odorata* were evaluated to hypothesized its wound healing mechanisms. The goal of this docking simulation is to predict the most likely binding interaction between the targeted wound healing protein and the plant's active ingredients (the ligands). This technique is very useful in the drug design since it allows screening of drug candidate prior to *in vitro* and *in vivo* analysis. In this docking study, the four topmost compounds (phytol, hexadecenoic acid ethyl ester, linolenic acid, and squalene) obtained by GC-MS analysis were docked against three wound healing target proteins.

Generally, wound healing process comprises of four distinctive stages namely haemostasis, inflammation, proliferation, and remodelling. The proteins selected for this investigation were acetylated human COX-2 (5F19),

Table 7. Drug-likeness and medicinal chemistry of selected compounds of *Chromolaena odorata*

Compound	Phytol	Hexadecanoic acid ethyl ester	Linolenic acid	Squalene
Lipinski #violations	Yes; 1 violation: MLOGP>4.15	Yes; 1 violation: MLOGP>4.15	Yes; 1 violation	Yes; 1 violation: MLOGP>4.15
Ghose #violations	No; 1 violation: WLOGP>5.6	No; 1 violation: WLOGP>5.6	No; 1 violation: WLOGP>5.6	No; 3 violations: WLOGP>5.6, MR>130, #atoms>70
Veber #violations	No; 1 violation: Rotors>10	No; 1 violation: Rotors>10	No; 1 violation: Rotors>10	No; 1 violation: Rotors>10
Egan #violations	No; 1 violation: WLOGP>5.88	No; 1 violation: WLOGP>5.88	No; 1 violation: WLOGP>5.88	No; 1 violation: WLOGP>5.88
Muegge #violations	No; 2 violations: XLOGP3>5, Heteroatoms<2	No; 2 violations: XLOGP3>5, Rotors>15	No; 2 violations: XLOGP3>5, Rotors>15	No; 2 violations: XLOGP3>5, Heteroatoms<2
Bioavailability Score	0.55	0.55	0.55	0.55
PAINS #alerts	0	0	0	0
Brenk #alerts	1 alert: isolated alkene	0	1 alert: isolated alkene	1 alert: isolated alkene
Lead-likeness	No; 2 violations: Rotors>7, XLOGP3>3.5	No; 2 violations: Rotors>7, XLOGP3>3.5	No; 2 violations: Rotors>7, XLOGP3>3.5	No; 3 violations: MW>350, Rotors>7, XLOGP3>3.5

GSK3-β (1Q5K), and MMP-9 (4H1Q) to represent inflammation, proliferation, and remodelling stages, respectively. These target proteins were selected as they have been reported to have significant role in wound healing process. All of the ligands-protein at their best docked position and interactions were presented based on their most stable binding energy (Table 8).

Interactions between the topmost compounds against COX-2 (5F19)

In the current work, the four topmost compounds were studies for their potentials as COX-2 inhibitors in promoting wound healing. The corresponding binding energy of COX-2 with phytol, hexadecanoic acid ethyl ester, linolenic acid, and squalene were -7.6 kcal/mol, -6.8 kcal/mol, -7.7 kcal/mol, and -8.6kcal/mol, respectively

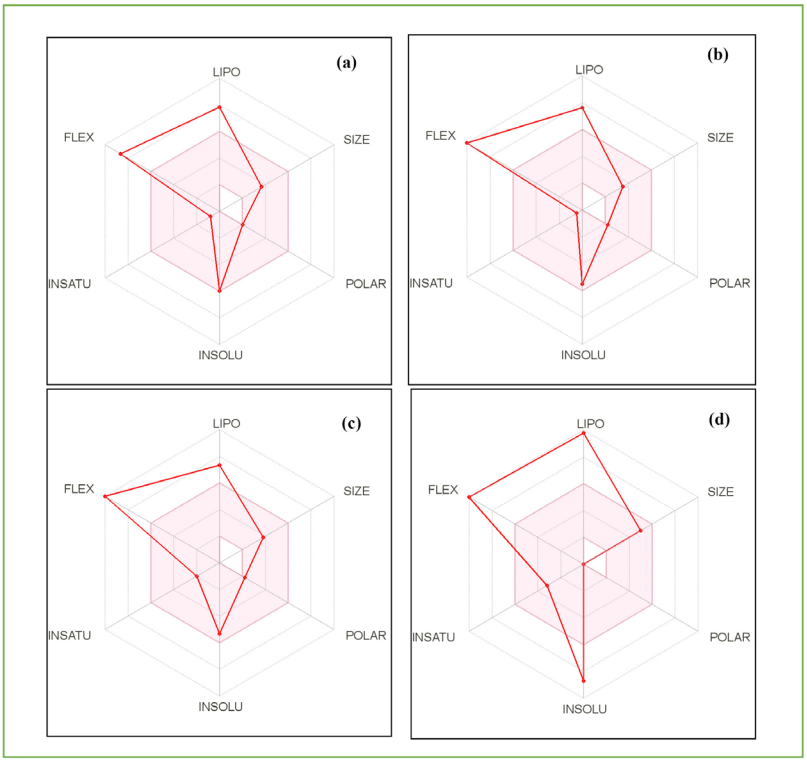

Figure 2. Bioavailability radar of selected compounds in *Chromolaena odorata*. (a) Phytol (b) Hexadecanoic acid ethyl ester (c) Linoenic acid, and (d) Squalene.

Table 8. Binding energy and molecular interactions of topmost compounds with different proteins (PDB ID: 5F19, 1Q5K, and 4H1Q)

Wound healing stage	Protein target	Compounds	Binding energy (kcal/mol)	H-bond	Hydrophobic bond
Inflammation	Acetylated human COX-2 (PDB ID: 5F19)	Phytol	-7.6	-	Phe205A, Leu534A, Tyr348A, Val523A, Val349A, Leu352A, Met522A, Phe518A, Trp387A, Gly526A, Ala527A, Leu384A, Tyr385A, Phe381A, Phe529A, Val228A, Phe209A, Gly533A, Leu531A
		Hexadecanoic acid	-6.8	-	Phe209A, Gly227A, Gly533A, Phe381A, Phe205A, Tyr385A, Ala527A, Gly526A, Val523A, Ser353A, Leu352A, Phe518A, Trp387A, Val344A, Val349A, Leu531A, Leu534A, Asn375A, Ile377A
		Linolenic acid	-7.7	Phe529A, Gly533A, Leu534A, Leu531A	Phe209A, Phe205A, Ala527A, Tyr385A, Phe381A, Gly526A, ValAL349A, Trp387A, Met522A, Leu352A, Val523A, Phe518A
		Squalene	-8.6	-	Val228A, Ile377A, Phe205A, Phe209A, Phe381A, Tyr385A, Gly526A, Ala527A, Trp387A, Leu352A, Phe518A, Val523A, Met522A, Tyr355A, Ser353A, Arg120A, Leu531A, Val349A, Val344A, Gly227A, Leu534A, Asn375A, Gly533A, Phe529A
Proliferation	GSK3-β (PDB ID: 1Q5K)	Phytol	-6.0	Pro1336A	Lys85A, Cys199A, Gly63A, Ala83A, Leu188A, Ile62A, Tyr134A, Glu137A, Val135A, Arg141A, Thr1338A, Val70A, Asn186A, Asp200A, Lys85A
		Hexadecanoic acid	-5.6	Phe67A, Ser66A	Val135A, Leu188A, Ala83A, Cys199A, Leu132A, Val70A, Ser66A, Asp200A, Asp264B, Lys85A, Gly65A
		Linolenic acid	-6.3	Val135A	Ala83A, Ile62A, LEU188A, Leu12A, Val70A, Tyr134A, Tyr140A, Gln185A, Arg141A, Thr138A, Glu137A
		Squalene	-6.8	-	Arg96A, Asn95A, Glu97A, Gly202A, Val87A, Phe67A, Pro294B, Ser66A, Val267B, Ala298B, Ile270B, Leu88A, Phe291B, Arg180A, Lys292B, Ile217A, Ser203A, Val263B
Remodelling	MMP-9 (PDB ID: 4H1Q)	Phytol	-7.1	Pro246A	Ala242B, Tyr245B, Leu243B, Leu222B, His226B, Thr251B, Tyr245A, Met247A, Arg249B, Tyr248B, Met247B, Gln227B, Val223B, Leu187B, Ala189B, Leu188B
		Hexadecanoic acid	-6.5	Arg249B	Met247A, Leu187B, Ala189B, Gln227B, Tyr248B, His226B, Val,223B, Pro255B, Leu222B, Ala242B, Leu243B, Met247B, Gly186B, Pro246A, Tyr245A, Leu188B
		Linolenic acid	-7.2	Met247B, Ala242B, Arg249B	Pro246A, Leu188B, His26B, Leu222B, Tyr248B, Leu243B, Val223B, Tyr245B, Pro246B, Tyr245A, His236B
		Squalene	-7.4	-	Ala242B, Pro255B, Leu243B, Arg249B, Tyr245B, Leu188B, Ala189B, Pro246B, Tyr245A, His236B, Leu187B, His230B, Gln227B, His226B, Val223B, Leu222B, Tyr248B, Thr251B, Met247B, Glu241B

(Table 8). A two-dimensional representation (Figure 3) visualized the interaction between the four compounds and the amino acid of COX-2. Only linolenic acid has shown hydrogen bond interaction with residues Phe529A, Gly533A, Leu534A, and Leu531A. The most stable binding of squalene shows hydrophobic interaction with residues Val228A, Ile377A, Phe205A, Phe209A, Phe381A, Tyr385A, Gly526A, Ala527A, Trp387A, Leu352A, Phe518A, Val523A, Met522A, Tyr355A, Ser353A, Arg120A, Leu531A, Val349A, Val344A, Gly227A, Leu534A, Asn375A, Gly533A, and Phe529A.

Interactions between topmost compounds against GSK3-β (1Q5K)

Based on the current docking simulation, squalene had the best binding energy score (-6.8 kcal/mol) as compared to other compounds tested. Through visualization of its molecular interactions (Figure 4), it was revealed that the all ligands interacted with GSK-3β through hydrophobic and hydrogen bonding interactions. Based on the results obtained, the ligands tested in this study showed molecular interactions with one or more amino acids in the active pockets of the binding site except for squalene as depicted in Table 8.

Remodeling stage of wound healing, MMP-9 (4H1Q)

Based on the current findings, squalene was found to have the best binding energy (-7.4 kcal/mL) towards MMP-9 as

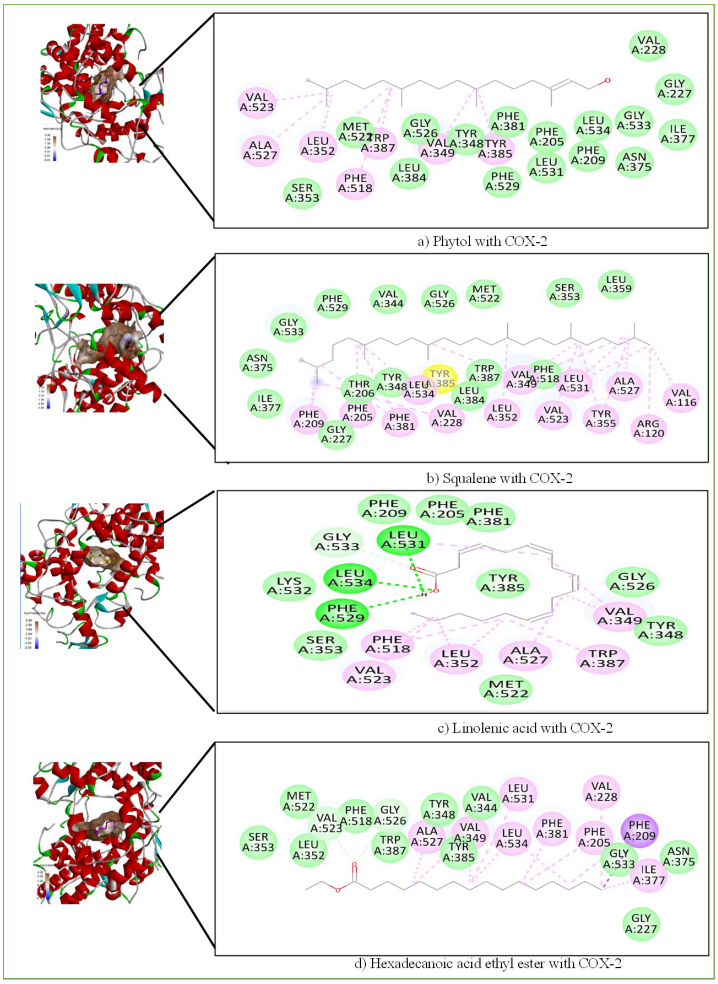

Figure 3. The topmost four compounds (stick representation) from *Chromolaena odorata* docked with COX-2. From 2D representation, the green dashed lines represent hydrogen bond, while other highlighted amino acid residues are hydrophobic bond.

compared to other compounds. The 2D interactions plot of protein indicated two types of interactions that exist, which are hydrophobic and hydrogen bond. Similar to the other target proteins 1Q5K (GSK3-β) and 5F19 (COX-2), hydrophobic bond was found to be the dominant type of interactions (Figure 5). Visualization of molecular interactions between MMP-9 and squalene revealed that the ligand interacted with Ala242B, Pro255B, Leu243B, Arg249B, Tyr245B, Leu188B, Ala189B, Pro246B, Tyr245A, His236B, Leu187B, His230B, Gln227B, His226B, Val223B, Leu222B, Tyr248B, Thr251B, Met247B, and Glu241B through hydrophobic contacts. Linolenic acid formed hydrophobic contacts with Pro246A, Leu188B, His26B, Leu222B, Tyr248B, Leu243B, Val223B, Tyr245B, Pro246B, Tyr245A, His236B and hydrogen bonds with Met247B, Ala242B, and Arg249B. On the other hand, phytol interacted with Ala242B, Tyr245B, Leu243B, Leu222B, His226B, Thr251B, Tyr245A, Met247A, Arg249B, Tyr248B, Met247B, Gln227B, Val223B, Leu187B, Ala189B, and Leu188B through hydrophobic contacts, and formed hydrogen bonds with Pro246A, and Pro246B. Hexadecenoic acid showed hydrophobic interactions with Met247A, Leu187B, Ala189B, Gln227B, Tyr248B, His226B, Val,223B, Pro255B, Leu222B, Ala242B, Leu243B, Met247B, Gly186B, Pro246A, Tyr245A, Leu188B and hydrogen bond with Arg249B.

Discussion

Chromolaena odorata possesses many secondary metabolites such as terpenes, alkaloids, and glycosides. Polyphenols like flavonoids and tannins are abundant in the Asteraceae family. Many of these phytochemicals possess various pharmacological activities useful to human wellness (24). Previous phytochemical studies on the extracts of *C. odorata* from various parts of the plant have indicated the presence of tannins, terpenoids, cardiac glycosides, saponins, anthraquinones, phenols, and alkaloids (25). About 44 different compounds have previously been isolated from *C. odorata* extracts using gas chromatography-mass spectrometry (26). Because of the presence of these phytochemicals, the plant is said to have anthelmintic (24), antioxidant (27), analgesic, anti-inflammatory, antipyretic, antispasmodic (28), antiacne (29), antimalarial, antioxidant, and wound healing properties (30). The phytochemical screening of

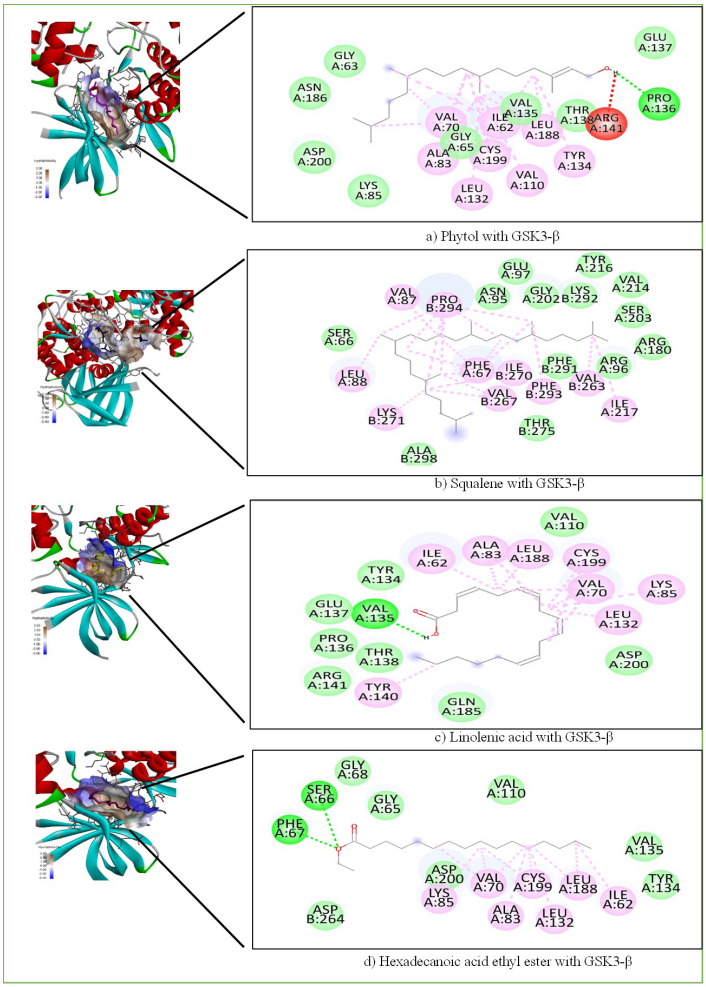

Figure 4. The topmost four compounds (stick representation) from *Chromolaena odorata* docked with GSK3-β. From 2D representation, the green dashed lines represent hydrogen bond, while other highlighted amino acid residues are hydrophobic bond.

C. odorata extract in this current work is in agreement with a previous reported (31). However, interestingly in the current study, phytol was found to be the most potent as compared to other compounds. Phytol had also being reported to be presented in *C. odorata* by previous works (26,31-32) but the amount was not as high as obtained in this study.

In order to develop and design new drugs, a thorough evaluation of drug candidates must be initially scrutinized for their pharmacokinetics properties. This includes the study on how a particular drug is ADME. Understanding and predicting the pharmacological rationale of traditional medicinal plants' therapeutic activity are important to upgrade their usage in modern medicine.

During early stage of drug development process, drug candidates are evaluated based on computer modelling, high-throughput screening, and cell-based tests that predict pharmacological action. Predicting drug ADME properties, which often require *in vivo* analysis, is substantially more difficult. Because *in vivo* studies are time consuming and costly, it is advantageous to have simple approaches in predicting ADME. An acknowledged strategy known as Lipinski's Rule of Five (RO5) is a widely used rule of thumb for predicting ADME properties of drugs in modern drug discovery, including plant phytoconstituents. The ADME prediction in this work was done using SwissADME web-based tool where RO5 was taken into account.

Based on this rule, for a particular drug candidate to be regard as a lead compound, the drug candidate should have less than 500 Da molecular weight (MW), less than 5 H-donor, less than 10 H-acceptor, and octanol-water partition coefficient (log P) that does not exceed 5. These criteria should not be violated more than one. However, based on a study conducted by Choy and Prausnitz (33) transdermal drug needs to have modified rules that are MW < 335 Da, H-donor < 2, H-acceptors < 5 and lop P <5.0.

Lipophilicity of a drug candidate molecule is a critical factor in developing its dosage form, as drug molecule must permeate the lipid bilayer of the majority of cellular membranes, including enterocytes. So it is commonly accepted that medication molecules must be lipophilic in order to be absorbed effectively. Based on the current

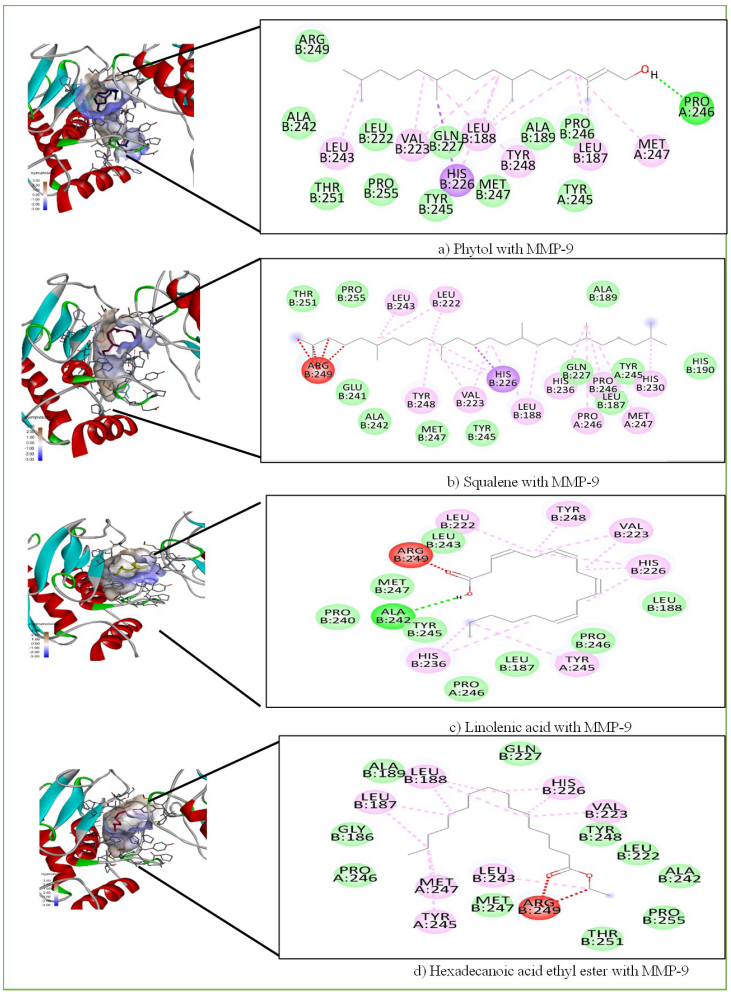

Figure 5. The topmost four compounds (stick representation) from *Chromolaena odorata* docked with MMP-9. From 2D representation, the green dashed lines represent hydrogen bond, while other highlighted amino acid residues are hydrophobic bond.

work, out of the four topmost compounds found in *C. odorata*, squalene showed to be the most lipophilic while hexadecanoic acid ethyl ester depicted as the least lipophilic activity. However, all compounds were still within the acceptable value of lipophilicity.

Pharmacokinetics evaluation of these compounds showed high gastrointestinal (GI) adsorption for hexadecanoic acid ethyl ester and linolenic acid while phytol and squalene exhibited low GI adsorption. All of the compounds showed no blood brain barrier (BBB) permeation. Among these four compounds assessed, only phytol showed to be a P-glycoprotein (P-gp) substrate. P-gp is one of the drug transporters that determine the uptake and efflux of drugs. Drugs which can induce or inhibit P-gp can interact with other drugs. P-gp is believed to be an important mediator of drug-drug interaction and hence need to be assessed for potential interaction when administered together (34).

The knowledge of interactions between compounds and the cytochrome P450 (CYP) system is very essential to characterize the pharmacokinetics of candidate drugs as these interactions are necessary for the transformation and elimination of the drugs from the system (23). Inhibitions of the isoforms of this enzyme system by drugs could results in poor elimination leading to drug-toxicity. Hence, it is important that a candidate drug has a limited inhibitory activity against these enzymes isoforms (23). In the current study, only squalene showed no potential to inhibit any of the five P450 isoforms, which indicates that this compound will be well-metabolized in the liver and eliminated easily from the body. Log Kp correlates with the ability of the compound under investigation to pass through the stratum corneum (skin) of mammalian cells. In SwissADME, the prediction of Log K_p was generated based on the linear model suggested by Potts and Guy (35). The more the negative the value of Log K_p, the less likely the compound to be absorbed in the skin. In the current study, squalene showed to have less negative value as compared to other compounds, which indicates that squalene has excellent absorption on the skin among all investigated compounds of *C. odorata*. These findings suggest that squalene should be further investigated for future potential transdermal drug candidate particularly in wound dressing formulations.

Another parameter in SwissADME tools is known as PAINS. PAINS is known as molecules that contain substructures showing potent response in assays irrespective of the protein target, which potentially can give false positive results in high-throughput screening (36). Common PAINS include toxoflavin, isothiazolones, hydroxyphenyl hydrazones, curcumin, phenol-sulfonamides, rhodanines, enones, quinones, and catechols (36,37). BRENK filter, on the other hand, is a structural alert that filters unwanted functionality due to potential toxicological reasons or unfavourable pharmacokinetics behaviour. These two descriptors (PAINS and BRENK) are important in helping medicinal chemists in selecting and judging promising drug candidates during pre-filtering or screening. In this present study, all of compounds had at least 1 alert for BRENK filter except for hexadecenoic acid ethyl ester. However, this result could not be deemed as final; there are several other criteria need to be taken into considerations when making decision on drug lead for further optimization. Bioavailability score represents the prediction of probability of a compound to have at least 10% oral bioavailability in rat or measurable $CaCO_2$ permeability (F>10%) based on the predominant charge at biological pH in rat models (38). In this study, all of the compounds investigated obtained 0.55 score, which is in compliance with Lipinski's RO5. A good drug-like molecule should have bioavailability score of 0.55-0.56 to be indicated as having good pharmacological behaviour (8). Also, based on the current study, all of the compounds are non-orally bioavailable for oral dosage form as they showed to be too flexible or high lipophile. This suggested that these compounds could be used to developed non-oral drugs (topical, ophthalmic, etc). Regardless bioavailability, drugs that are intended to be developed should have good absorption, distribution, metabolism and excretion from the body system and these are achieved through early assessment using this SwissADME tool.

In this direction, the topmost active ingredients of *C. odorata*, were further evaluated through molecular docking approach to hypothesize its wound healing mechanisms. The goal of this docking simulation was to predict the most likely binding interaction between the targeted wound healing protein and the plant's active ingredients (the ligands). This technique is very useful in drug design, since it allows screening of drug candidate prior to *in vitro* and *in vivo* analysis. In this docking study, the four topmost compounds (phytol, hexadecenoic acid ethyl ester, linolenic acid, and squalene) obtained by GC-MS analysis were docked against three wound healing target proteins.

During inflammation stages of wound healing, inhibition of COX-2 activity has been reported to reduce wound inflammation and promote dermal reconstruction and scar formation (39). In support of this claim, another study (40) inferred that COX-2 inhibition did not alter the baseline repair outcomes of the biological scaffold therapy. This strengthens the rationale for selective COX-2 inhibition as wound repair target does not interfere with wound healing cascade. Interestingly, as compared to other protein targets studied in the present work, COX-2 possessed the most stable binding towards *C. odorata's* topmost compounds. The hydrophobic effect plays an important role in this protein ligand binding. The binding site with more hydrophobic substituent increases the binding affinity. Thus, it can be proposed that hydrophobic interaction might influence the best inhibition effect towards the target protein. Hydrophobic interaction and hydrogen bonds are among the most frequently observed interactions and widely used in drug design (41). Ferreira de Freitas and Schapira (41) mentioned that hydrophobic interactions are more frequent in high-efficiency ligands in drug-receptor interactions. It is a prevailing directional molecular interaction in biological complexes and a predominant contribution to the specificity of molecular recognition (41). Previous studies have discovered that there are several amino acid residues found in the ligand binding pocket, including Ile62, Gly63, Val70, Tyr71, Gln72, Ala73, Leu81, Val82, Ala83, Ile84, Lys85, Val110, Leu132, Asp133, Tyr134, Val135, Pro136, Glu137, Thr138, Arg141, Gln185, Asn186, Leu187, Leu188, Leu189, Asp190 and Lys197 (12,18,42).

The Wnt/β-catenin pathway is a highly conserved signal transduction pathway involved in a variety of biological processes, such as cell proliferation, apoptosis, and differentiation. In wound healing process, it was proven that upregulation of β-catenin through the activation of Wnt/β-catenin signaling pathway can help accelerate wound healing (43). One of the strategy to activate this pathway is through the inhibition of GSK-3β (43). Considering the role of the Wnt/β-catenin is recently used as an important target for the development of wound-healing agents. Molecules that can activate the Wnt/β-catenin pathway are evaluated by researchers as potential therapeutics in wound healing (44).

In the current work, we aimed to elucidate the potential of four topmost *C. odorata*'s compounds as GSK-3β inhibitors by looking at their binding interaction towards the target protein. Presumably, molecules with the lowest docking scores are considered as the best molecules to inhibit the target receptor because lower docking score indicates stable binding affinity (45).

MMP-9, a form of collagenase, is also a primary culprit for causing delayed wound healing process. Various studies have discovered the elevated levels of MMP-9 in chronic wound patients (46). According to Reiss et al (47), MMP-9 is the causal factor that is responsible for the development of chronic wounds. In addition, it has been reported that higher MMP-9 levels can cause delay in collagen deposition of alveolar

bone repair. Therefore, MMP-9 has also been aimed as molecular target for wound healing, and numerous efforts have been made to develop MMP-9 inhibitors. Peng et al (48) demonstrated that selective inhibition of MMP-9 in mice could significantly accelerate wound healing. Similarly, in the current study, we aimed to explore the potential of these four compounds as MMP-9 inhibitors. The stability of the protein-ligand complex depends on the strong interaction between the interacting subunits (13). Previous analysis conducted on a large amounts of experimental data disclosed that hydrophobic interactions and hydrogen bonds contribute the most to the stability of protein folding (13). By observing the binding affinity and molecular interactions of the selected ligands with MMP-9 protein, it is suggested that these topmost compounds of *C. odorata* might be potential inhibitors for MMP-9 protein.

Conclusion

In the current work, preliminary phytochemical screening of *C. odorata* extract showed the presence of several secondary metabolites, including terpenoids, steroids, flavonoids, alkaloids, saponin, and tannins. Further elucidation of the phytochemicals via GC-MS revealed that the most abundant compounds were phytol (49.83%), hexadecanoic acid ethyl ester (9.40%), linolenic acid (8.07%), and squalene (3.53%). Pharmacokinetic study through ADME analysis revealed that in general all four topmost compounds obeyed Lipinski's Rule of 5. This give the idea for further investigation of these compounds to be optimized as lead compounds in drug discovery. *In silico* molecular docking study of these top phytoconstituents against several protein targets involved in wound healing revealed that squalene had the highest binding affinity to GSK3β (-6.8 kJ/mol), MMP-9 (-7.4 kJ/mol), and COX-2 (-8.6 kJ/mol) as compared to other ligands (phytol, linolenic acid, and hexadecenoic acid ethyl ester). Among four compounds tested, squalene showed the strongest binding towards all of the target proteins. Also, based on the current work, it is suggested that these compounds have higher wound healing activity during inflammation stage as they portrayed the lowest energy binding towards COX-2 target protein as compared to GSK-3β and MMP-9. This finding also suggested that the most prominent compound that contributes to *C. odorata's* wound healing capacity was squalene, and incorporation of *C. odorata* in potential agent in wound dressing formulation was justified. However, further study should be conducted to isolate the compounds of interest from the crude extract.

Acknowledgement

All authors would like to thanks supporting staffs in Universiti Teknologi Malaysia, International Campus, Kuala Lumpur for technical supports throughout the project.

Authors' contributions

All authors have equally contributed to all aspects of the manuscripts. NAM conceived the idea and data collections, developed the article, wrote and prepared the manuscript. FMT and NHMR conducted and analyzed the molecular docking work. NBAK and RRA supervised the research and critical revision of the article. All authors read the manuscript and confirmed the publication of the final version.

Conflict of interests

Authors declared no conflict of interests.

Ethical considerations

Ethical issues regarding authorship, data acquisition, visualization and analysis have been carefully experiential and reviewed by all authors.

Funding/Support

PhD scholarship to Nur 'Ainun Mokhtar (BS860521566430) is gratefully acknowledge.

References

1. Sen CK. Human wounds and its burden: an updated compendium of estimates. Adv Wound Care (New Rochelle). 2019;8(2):39-48. doi: 10.1089/wound.2019.0946.
2. Vaisakh MN, Pandey A. The invasive weed with healing properties: a review on *Chromolaena odorata*. Int J Pharm Sci Res. 2012;3(1):80-3.
3. Kumarasamyraja D, Jeganathan NS, Manavalan R. A review on medicinal plants with potential wound healing activity. Int J Pharma Sci. 2012;2(4):101-7.
4. Keskes H, Belhadj S, Jlail L, El Feki A, Damak M, Sayadi S, et al. LC-MS-MS and GC-MS analyses of biologically active extracts and fractions from Tunisian *Juniperus phoenice* leaves. Pharm Biol. 2017;55(1):88-95. doi: 10.1080/13880209.2016.1230139.
5. Fang J, Liu C, Wang Q, Lin P, Cheng F. In silico polypharmacology of natural products. Brief Bioinform. 2018;19(6):1153-71. doi: 10.1093/bib/bbx045.
6. Loza-Mejía MA, Salazar JR, Sánchez-Tejeda JF. In silico studies on compounds derived from *Calceolaria*: phenylethanoid glycosides as potential multitarget inhibitors for the development of pesticides. Biomolecules. 2018;8(4):121. doi: 10.3390/biom8040121.
7. Lee K, Kim D. In-silico molecular binding prediction for human drug targets using deep neural multi-task learning. Genes (Basel). 2019;10(11):906. doi: 10.3390/genes10110906.
8. Bojarska J, Remko M, Breza M, Madura ID, Kaczmarek K, Zabrocki J, et al. A supramolecular approach to structure-based design with a focus on synthons hierarchy in ornithine-derived ligands: review, synthesis, experimental and in silico studies. Molecules. 2020;25(5):1135. doi: 10.3390/molecules25051135.
9. Moeller MJ, Soofi A, Braun GS, Li X, Watzl C, Kriz W, et al. Protocadherin FAT1 binds Ena/VASP proteins and is necessary for actin dynamics and cell polarization. EMBO

J. 2004;23(19):3769-79. doi: 10.1038/sj.emboj.7600380.
10. Leelananda SP, Lindert S. Computational methods in drug discovery. Beilstein J Org Chem. 2016;12:2694-718. doi: 10.3762/bjoc.12.267.
11. Reshad RAI, Alam S, Raihan HB, Meem KN, Rahman F, Zahid F, et al. In silico investigations on curcuminoids from *Curcuma longa* as positive regulators of the Wnt/β-catenin signaling pathway in wound healing. bioRxiv [Preprint]. April 4, 2020. Available from: https://www.biorxiv.org/content/10.1101/2020.03.19.998286v2.
12. Bailly C, Vergoten G. Molecular docking study of xylogranatins binding to glycogen synthase kinase-3β. Digit Chin Med. 2022;5(1):9-17. doi: 10.1016/j.dcmed.2022.03.002.
13. Afriza D, Orienty FN, Ayu WP. Molecular docking analysis of the interactions between MMP-9 protein and four coumarin compounds (nordentatin, dentatin, calusenidin and xanthoxyletin). J Int Dent Med Res. 2020;13(4):1286-92.
14. Narayanaswamy R, Wai LK, Esa NM. Molecular docking analysis of phytic acid and 4-hydroxyisoleucine as cyclooxygenase-2, microsomal prostaglandin E synthase-2, tyrosinase, human neutrophil elastase, matrix metalloproteinase-2 and -9, xanthine oxidase, squalene synthase, nitric oxide synthase, human aldose reductase, and lipoxygenase inhibitors. Pharmacogn Mag. 2017;13(Suppl 3):S512-S8. doi: 10.4103/pm.pm_195_16.
15. Tamboli FA, More HN. In vitro antipsoriatic study of successive solvent extracts of *Barleria gibsoni* Dalz. using HaCa T keratinocyte cells. Res J Pharm Technol. 2015;8(11):1566-9. doi: 10.5958/0974-360x.2015.00279.6.
16. Futagami A, Ishizaki M, Fukuda Y, Kawana S, Yamanaka N. Wound healing involves induction of cyclooxygenase-2 expression in rat skin. Lab Invest. 2002;82(11):1503-13. doi: 10.1097/01.lab.0000035024.75914.39.
17. Hariono M, Yuliani SH, Istyastono EP, Riswanto FDO, Adhipandito CF. Matrix metalloproteinase 9 (MMP9) in wound healing of diabetic foot ulcer: molecular target and structure-based drug design. Wound Med. 2018;22:1-13. doi: 10.1016/j.wndm.2018.05.003.
18. Harish BG, Krishna V, Santosh Kumar HS, Khadeer Ahamed BM, Sharath R, Kumara Swamy HM. Wound healing activity and docking of glycogen-synthase-kinase-3-beta-protein with isolated triterpenoid lupeol in rats. Phytomedicine. 2008;15(9):763-7. doi: 10.1016/j.phymed.2007.11.017.
19. Valdés-Tresanco MS, Valdés-Tresanco ME, Valiente PA, Moreno E. AMDock: a versatile graphical tool for assisting molecular docking with Autodock Vina and Autodock4. Biol Direct. 2020;15(1):12. doi: 10.1186/s13062-020-00267-2.
20. Tonzibo ZF, Wognin E, Chalchat JC, N'Guessan YT. Chemical investigation of *Chromolaena odorata* L. King Robinson from ivory coast. J Essent Oil Bear Plants. 2007;10(2):94-100. doi: 10.1080/0972060x.2007.10643525.
21. Pitakpawasutthi Y, Thitikornpong W, Palanuvej C, Ruangrungsi N. Chlorogenic acid content, essential oil compositions, and in vitro antioxidant activities of *Chromolaena odorata* leaves. J Adv Pharm Technol Res. 2016;7(2):37-42. doi: 10.4103/2231-4040.177200.
22. Ononamadu CJ, Ibrahim A. Molecular docking and prediction of ADME/drug-likeness properties of potentially active antidiabetic compounds isolated from aqueous-methanol extracts of *Gymnema sylvestre* and *Combretum micranthum*. BioTechnologia (Pozn). 2021;102(1):85-99. doi: 10.5114/bta.2021.103765.
23. Daina A, Michielin O, Zoete V. SwissADME: a free web tool to evaluate pharmacokinetics, drug-likeness and medicinal chemistry friendliness of small molecules. Sci Rep. 2017;7:42717. doi: 10.1038/srep42717.
24. Panda D, Dash SK, Dash GK. Qualitative phytochemical analysis and investigation of anthelmintic and wound healing potentials of various extracts of *Chromolaena odorata* Linn. collected from the locality of Mohuda village, Berhampur (South Orissa). Int J Pharm Sci Rev Res. 2010;1(2):122-6.
25. Vijayaraghavan K, Rajkumar J, Bukhari SN, Al-Sayed B, Seyed MA. *Chromolaena odorata*: a neglected weed with a wide spectrum of pharmacological activities. Mol Med Rep. 2017;15(3):1007-16. doi: 10.3892/mmr.2017.6133.
26. Venkata Raman B, Samuel LA, Pardha Saradhi M, Narashimha Rao B, Naga Vamsi Krishna A, Sudhakar M, et al. Antibacterial, antioxidant activity and GC-MS analysis of *Eupatorium odoratum*. Asian J Pharm Clin Res. 2012;5(2):99-106.
27. Vijayaraghavan K, Ali SM, Maruthi R. Studies on phytochemical screening and antioxidant activity of *Chromolaena odorata* and *Annona squamosa*. Int J Innov Res Sci Eng Technol. 2013;2(12):7315-21.
28. Chakraborty AK, Rambhade S, Patil UK. *Chromolaena odorata* (L.): an overview. J Pharm Res. 2011;4(3):573-6.
29. Chomnawang MT, Surassmo S, Nukoolkarn VS, Gritsanapan W. Antimicrobial effects of Thai medicinal plants against acne-inducing bacteria. J Ethnopharmacol. 2005;101(1-3):330-3. doi: 10.1016/j.jep.2005.04.038.
30. Anyasor GN, Aina DA, Olushola M, Aniyikaye AF. Phytochemical constituent, proximate analysis, antioxidant, antibacterial and wound healing properties of leaf extracts of *Chromolaena odorata*. Ann Biol Res. 2011;2(2):441-51.
31. Jumaat SR, Tajuddin SN, Sudmoon R, Chaveerach A, Abdullah UH, Mohamed R. Chemical constituents and toxicity screening of three aromatic plant species from Peninsular Malaysia. BioResources. 2017;12(3):5878-95. doi: 10.15376/biores.12.3.5878-5895.
32. Lawal O, Opoku A, Ogunwande I. Phytoconstituents and insecticidal activity of different solvent leaf extracts of *Chromolaena odorata* L., against *Sitophilus zeamais* (Coleoptera: Curculionidae). European J Med Plants. 2015;5(3):237-47. doi: 10.9734/ejmp/2015/6739.
33. Choy YB, Prausnitz MR. The rule of five for non-oral routes of drug delivery: ophthalmic, inhalation and transdermal. Pharm Res. 2011;28(5):943-8. doi: 10.1007/s11095-010-0292-6.
34. Lin JH, Yamazaki M. Role of P-glycoprotein in pharmacokinetics: clinical implications. Clin Pharmacokinet. 2003;42(1):59-98. doi: 10.2165/00003088-200342010-00003.
35. Potts RO, Guy RH. Predicting skin permeability. Pharm Res. 1992;9(5):663-9. doi: 10.1023/a:1015810312465.
36. Baell JB, Holloway GA. New substructure filters for removal of pan assay interference compounds (PAINS) from

screening libraries and for their exclusion in bioassays. J Med Chem. 2010;53(7):2719-40. doi: 10.1021/jm901137j.
37. Baell J, Walters MA. Chemistry: chemical con artists foil drug discovery. Nature. 2014;513(7519):481-3. doi: 10.1038/513481a.
38. Mahanthesh MT, Ranjith D, Yaligar R, Jyothi R, Narappa G, Ravi MV. Swiss ADME prediction of phytochemicals present in *Butea monosperma* (Lam.) Taub. J Pharmacogn Phytochem. 2020;9(3):1799-809.
39. Romana-Souza B, Dos Santos JS, Bandeira LG, Monte-Alto-Costa A. Selective inhibition of COX-2 improves cutaneous wound healing of pressure ulcers in mice through reduction of iNOS expression. Life Sci. 2016;153:82-92. doi: 10.1016/j.lfs.2016.04.017.
40. Goldman SM, Valerio MS, Janakiram NB, Dearth CL. COX-2 inhibition does not alter wound healing outcomes of a volumetric muscle loss injury treated with a biologic scaffold. J Tissue Eng Regen Med. 2020;14(12):1929-38. doi: 10.1002/term.3144.
41. Ferreira de Freitas R, Schapira M. A systematic analysis of atomic protein-ligand interactions in the PDB. Medchemcomm. 2017;8(10):1970-81. doi: 10.1039/c7md00381a.
42. Raja Naika H, Krishna V, Lingaraju K, Chandramohan V, Dammalli M, Navya PN, et al. Molecular docking and dynamic studies of bioactive compounds from *Naravelia zeylanica* (L.) DC against glycogen synthase kinase-3β protein. J Taibah Univ Sci. 2015;9(1):41-9. doi: 10.1016/j.jtusci.2014.04.009.
43. Choi S, Yoon M, Choi KY. Approaches for regenerative healing of cutaneous wound with an emphasis on strategies activating the Wnt/β-catenin pathway. Adv Wound Care (New Rochelle). 2022;11(2):70-86. doi: 10.1089/wound.2020.1284. 4
44. Shi H, Zhou C, He P, Huang S, Duan Y, Wang X, et al. Successful treatment with plasma exchange followed by intravenous immunoglobulin in a critically ill patient with COVID-19. Int J Antimicrob Agents. 2020;56(2):105974. doi: 10.1016/j.ijantimicag.2020.105974.
45. Simon L, Imane A, Srinivasan KK, Pathak L, Daoud I. In silico drug-designing studies on flavanoids as anticolon cancer agents: pharmacophore mapping, molecular docking, and Monte Carlo method-based QSAR modeling. Interdiscip Sci. 2017;9(3):445-58. doi: 10.1007/s12539-016-0169-4.
46. Nguyen TT, Mobashery S, Chang M. Roles of matrix metalloproteinases in cutaneous wound healing. In: Alexandrescu VA, ed. Wound Healing-New Insights into Ancient Challenges. IntechOpen; 2016. p. 37-71. doi: 10.5772/64611.
47. Reiss MJ, Han YP, Garcia E, Goldberg M, Yu H, Garner WL. Matrix metalloproteinase-9 delays wound healing in a murine wound model. Surgery. 2010;147(2):295-302. doi: 10.1016/j.surg.2009.10.016.
48. Peng Z, Nguyen TT, Song W, Anderson B, Wolter WR, Schroeder VA, et al. Selective MMP-9 inhibitor (R)-ND-336 alone or in combination with linezolid accelerates wound healing in infected diabetic mice. ACS Pharmacol Transl Sci. 2021;4(1):107-17. doi: 10.1021/acsptsci.0c00104